Open charm Spectroscopy and exotic states at LHCb.

Antimo Palano
INFN and University of Bari, Italy
On behalf of the LHCb Collaboration

Outline:

- New results on charm spectroscopy.
- Determination of the quantum numbers of X(3872)

The 7th International Workshop on Charm Physics, CHARM 2015, May 18, 2015, Detroit

The LHCb experiment.

- ☐ LHCb experiment is collecting very large samples of $c\bar{c}$ and $b\bar{b}$ events (JINST 3 (2008)S08005).

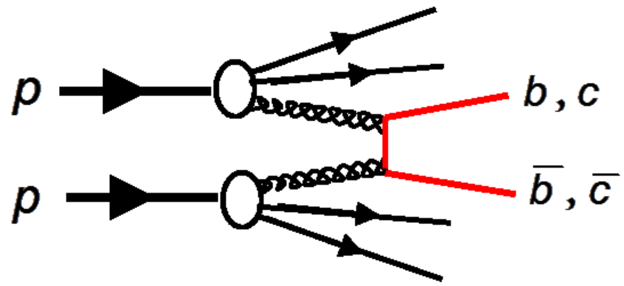

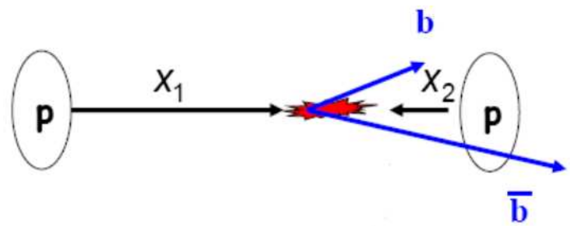

$\sigma(b\bar{b})$ $\quad$ *at 7 TeV* $\approx 290\ \mu b$

$\sigma(c\bar{c}) \approx 20 \times \sigma(b\bar{b})$

Nuclear Physics, Section B 871 (2013))

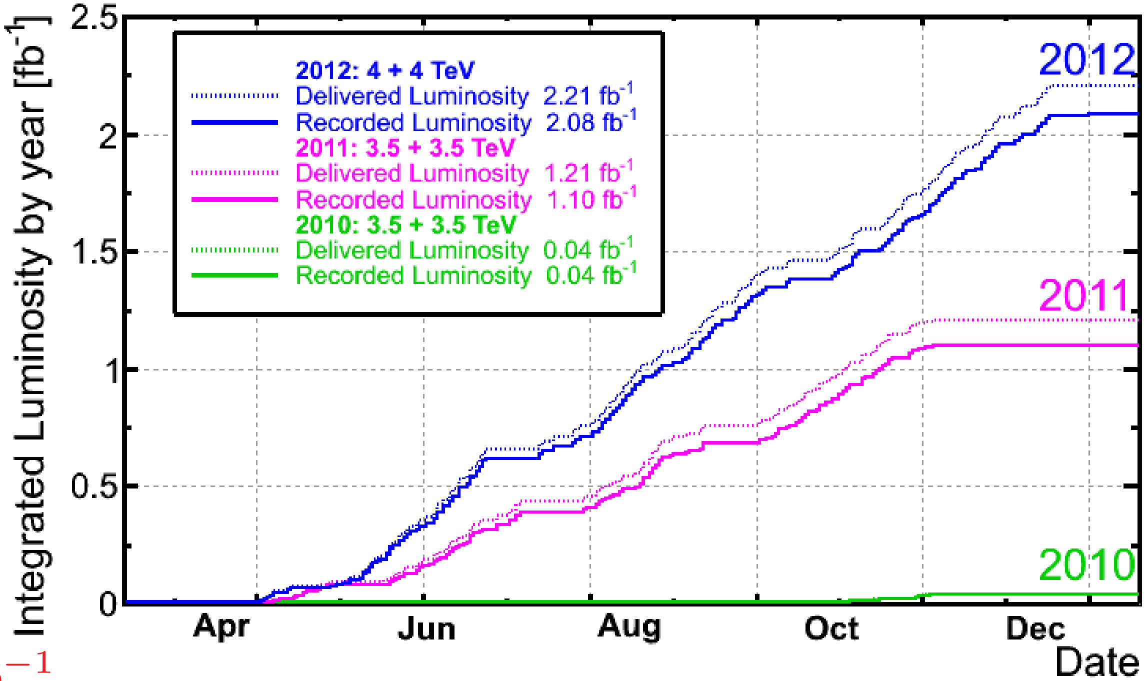

- ☐ Collected for Physics $\approx 3.0\ fb^{-1}$.

The LHCb experiment.

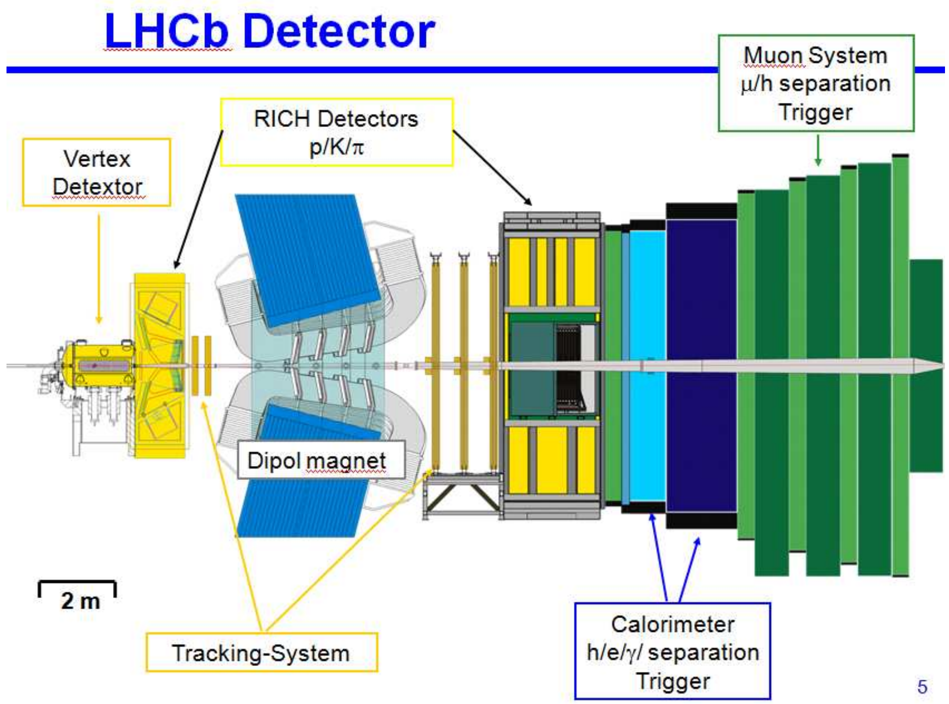

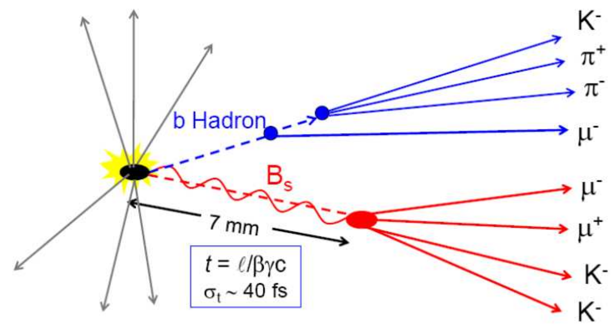

- □ Precise reconstruction of primary and secondary vertices.
- □ Accurate mass measurements of charm and beauty.
- □ Excellent K/π separation (K identification efficiency = 95% with 5% of pion misidentification).
- □ All type of B hadrons produced:($B^{\pm}$, B^0, B^0_s, b-baryons, $B^{\pm}_c$).
- □ Main issue for B and charm physics is the large vertex separation. Big boost, long-lived particles fly over long distances. Easy secondary vertex separation.

Charm meson spectroscopy

□ The quark model predicts many states with different quantum numbers in limited mass regions (Godfrey and Isgur, Phys.Rev.D32,189 (1985)).

□ In red are shown the established states

□ The ground states (D, D^*), and two of the 1P states, $D_1(2420)$ and $D_2^*(2460)$ are experimentally well established since they have relatively narrow widths ($\sim$30 MeV).

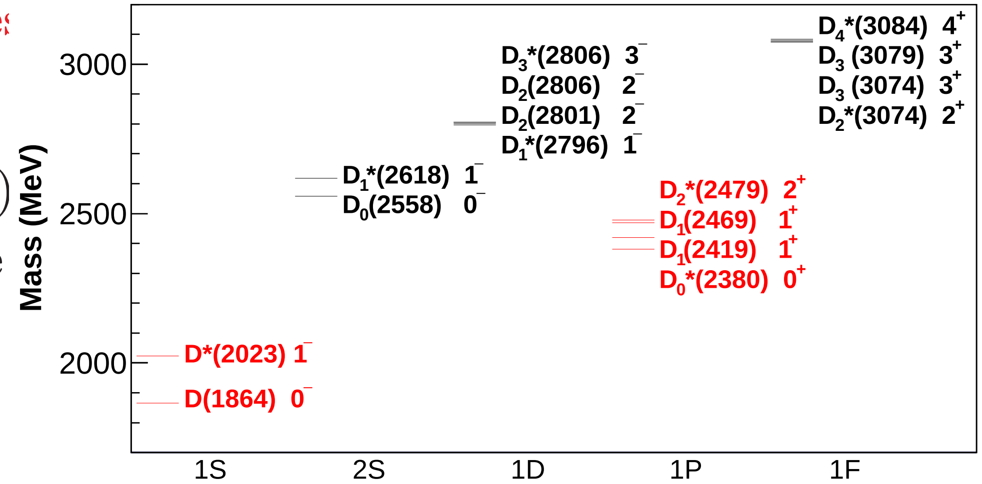

□ New progress in the understanding of the D_J spectrum come from:

- Inclusive studies of $D^0\pi^+$, $D^+\pi^-$ and $D^{*+}\pi^-$ from BaBar (Phys.Rev.D82:111101,(2010));

$$\boxed{e^+e^- \to D_J X}$$

- Inclusive studies of $D^0\pi^+$, $D^+\pi^-$ and $D^{*+}\pi^-$ from LHCb (JHEP09 (2013), 145);

$$\boxed{pp \to D_J X}$$

- New: Exclusive studies in Dalitz plot analyses of B decays from LHCb.

Charm meson spectroscopy

- Recent experimental status of the D_J spectroscopy.
- In black are shown the new states.
- Tentative assignments.

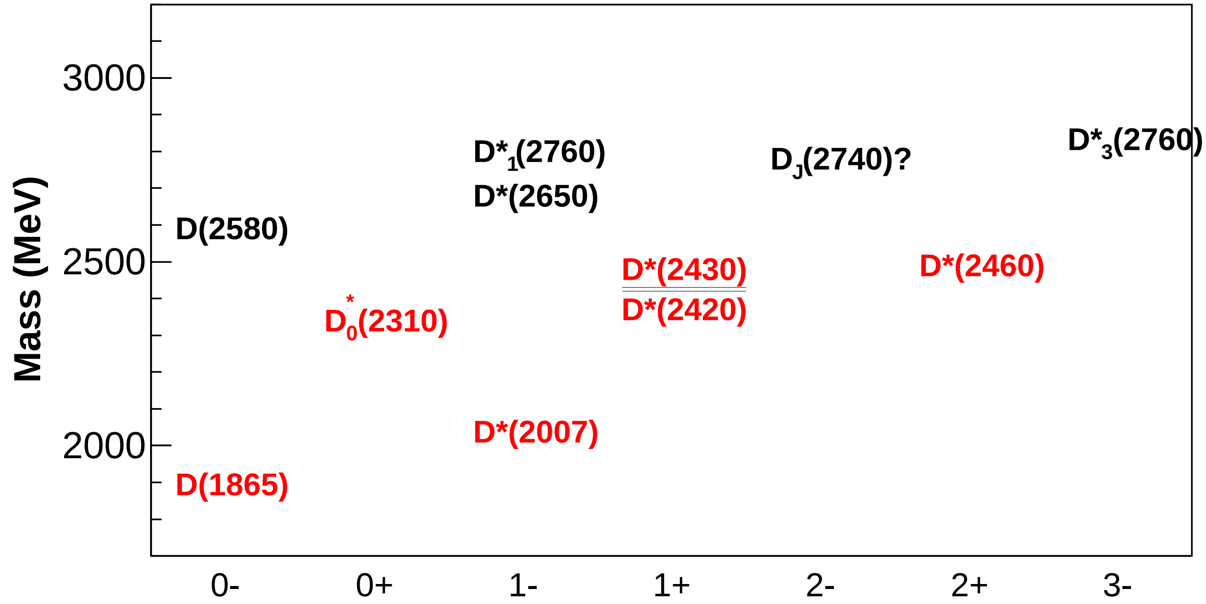

- States having $J^P = 0^+, 1^-, 2^+, 3^-, ..$ are defined as having "Natural Parity".
- States having $J^P = 0^-, 1^+, 2^-, ...$ are defined as having "Unnatural Parity".
- A resonance decaying to $D\pi$ has "Natural Parity". Labelled with D^*.
- The $D^*\pi$ system can access to both "Natural Parity" and "Unnatural Parity", except for $J^P = 0^+$ which is forbidden.

Two new Natural Parity states.

□ The $D^*(2610)/D^*(2650)$ and $D^*(2760)$ candidates for being the $J^P = 1^-$ $D_1^3(2S)$ and $J^P = 1^-$ $D_1^3(1D)$.

□ Observed in $D\pi$ and $D^*\pi$.

□ $D^{*+}\pi^-$ and $D^0\pi^+$ mass spectra from LHCb ($1\ fb^{-1}$)(JHEP09 (2013), 145).

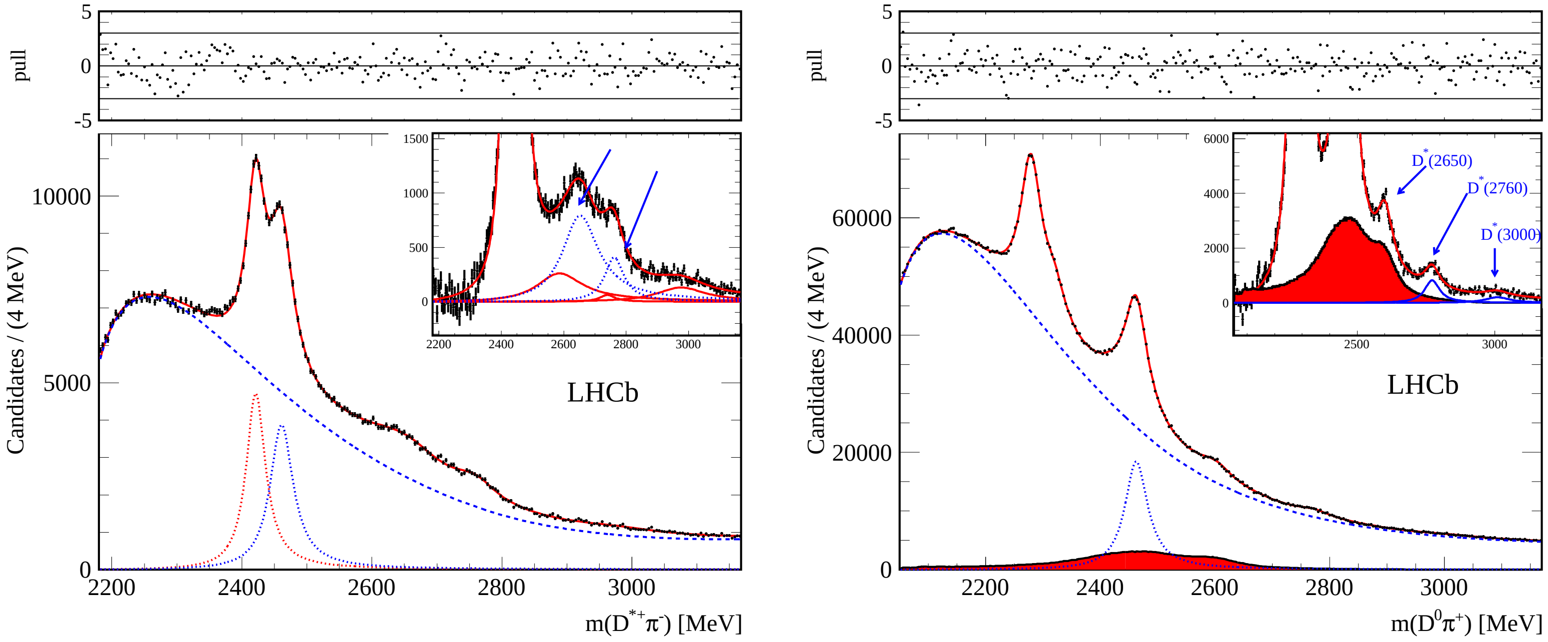

□ Note the crossfeed from the high mass D_J resonances into the $D\pi$ mass spectra.

□ This may explain the difference in the $D^*(2610)/D^*(2650)$ parameters between BaBar and LHCb.

Two new Natural Parity states.

- Plot of the different parameters measurements. BaBar in black, LHCb in red.
- Statistical and systematic uncertainties added in quadrature.

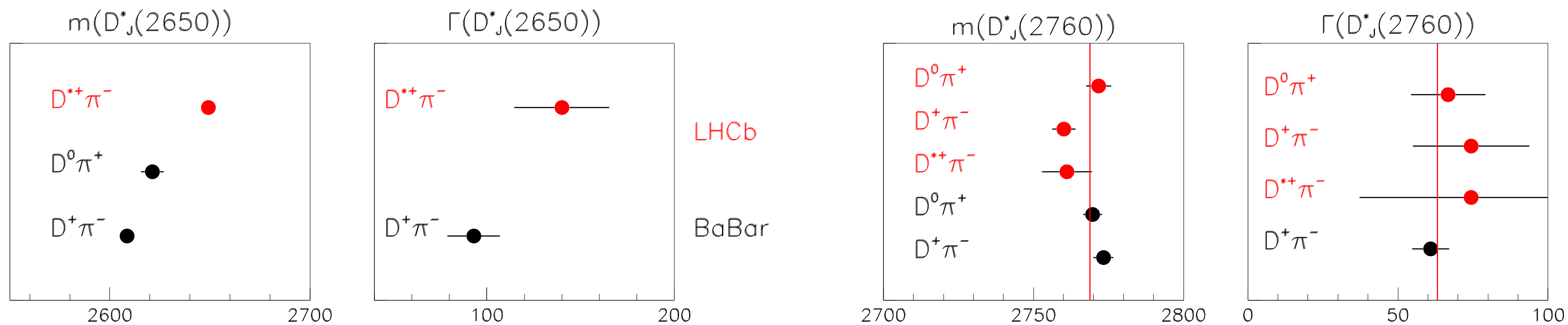

- Weighted mean values for $D^*_J(2770)$ parameters.

$$m(D_J(2770)) = 2768.8 \pm 1.7\ MeV, \qquad \Gamma(D_J(2770)) = 63.2 \pm 5.3\ MeV$$

- Angular distributions for $D^*_J(2650)$ and $D^*(2760)$ $(1\ fb^{-1})$(JHEP09 (2013), 145).

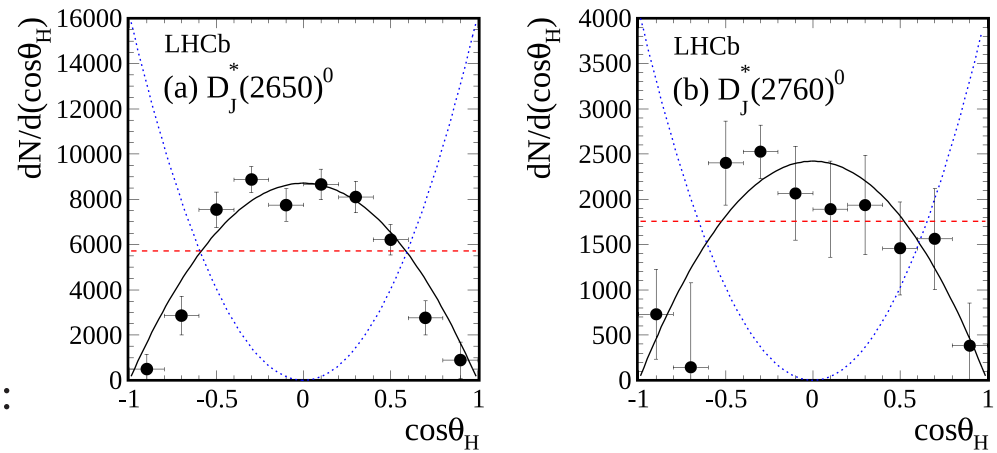

- Consistent with having Natural Parity: fitted with $sin^2\theta_H$.

Two/three new Unnatural Parity states.

□ Angular distributions for $D_J(2580)^0$, $D_J(2740)^0$, and $D_J(3000)^0$.

(black: natural parity), *(dashed red: unnatural parity)*, *(dotted blue: $J^P = 0^-$)*

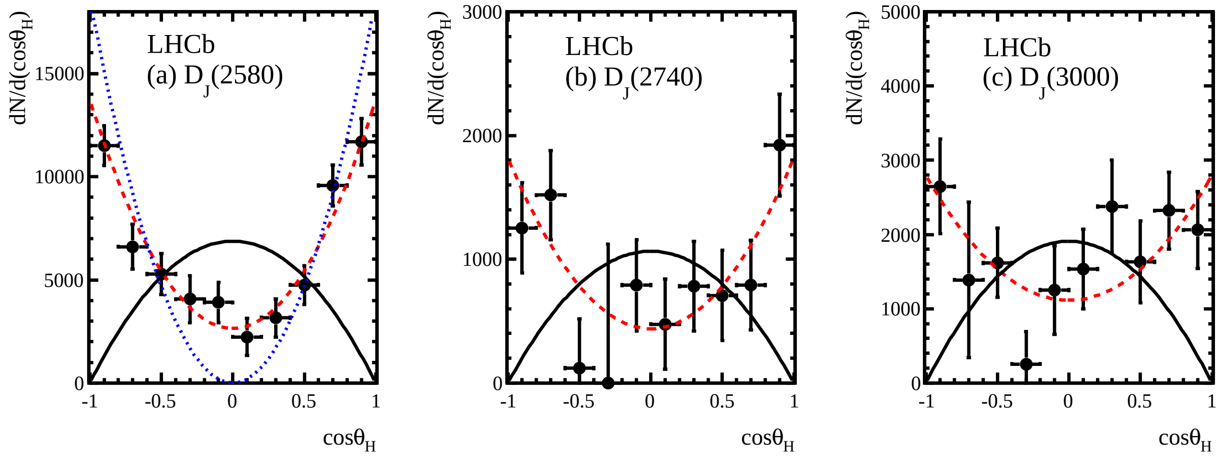

□ Weighted mean values for $D_J(2580)$ parameters.

$$m(D_J(2580)) = 2564.0 \pm 5.1\ MeV, \qquad \Gamma(D_J(2580)) = 135.6 \pm 16.9\ MeV$$

□ In Babar analysis fitted well with $J^P = 0^-$.

□ Weighted mean values for $D_J(2740)$ parameters.

$$m(D_J(2740)) = 2751.3 \pm 3.1\ MeV, \qquad \Gamma(D_J(2740)) = 71.4 \pm 11.4\ MeV$$

□ Candidate for $J^P = 2^-$.

□ Broad structures in the 3000 MeV mass region. Superposition of several states?

First observation and Dalitz plot analysis of $B^- \to D^+ K^- \pi^-$

(arXiv:1503.02995)

- The $D^+ K^- \pi^-$ mass spectrum contains $\approx 2K$ events in the B^- signal region.
- Integrated luminosity: $3\ fb^{-1}$.

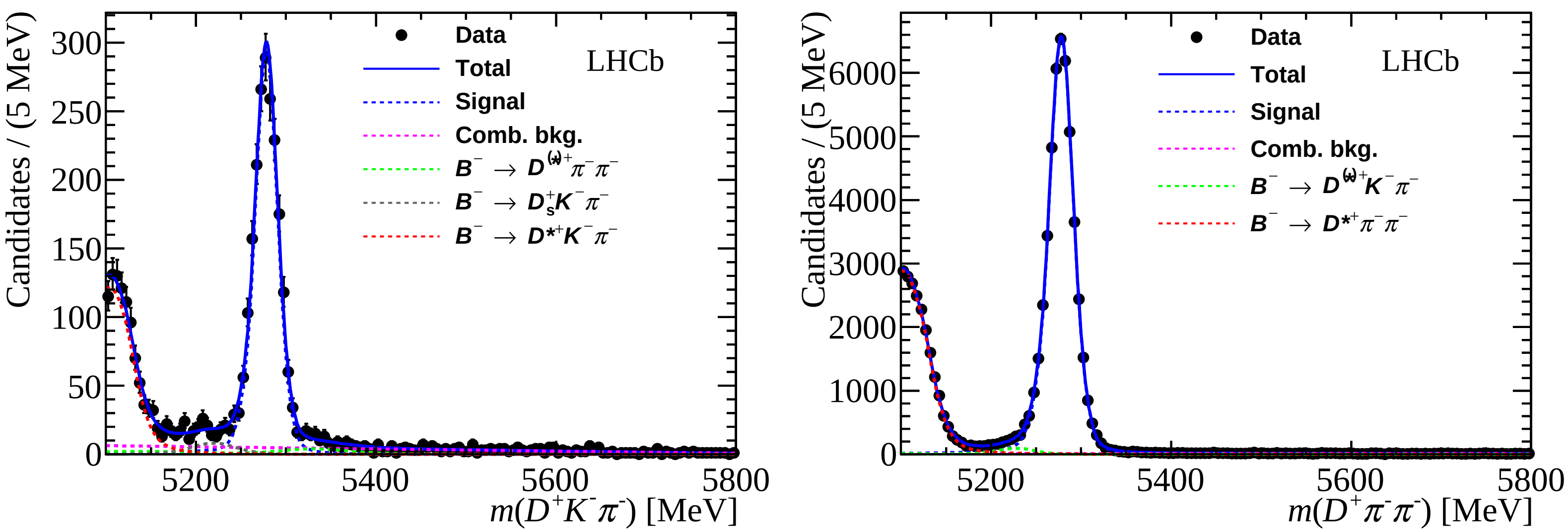

- Use of neural network's trained by control samples, especially $B^- \to D^+ \pi^- \pi^-$ ($\approx 49K$ events).

Partial wave analysis of the $D^+\pi^-$ system.

- In $B^- \to D^+K^-\pi^-$, resonance production can only occur in the $D^+\pi^-$ system (arXiv:1503.02995).
- Efficiency corrected and background subtracted $D^+\pi^-$ mass spectrum, weighted by Legendre polynomial moments
- Comparison with Dalitz plot fit results.
- If we consider only contributions up to spin 2, (h_0, h_1, h_2 indicate S-,P-,D-waves

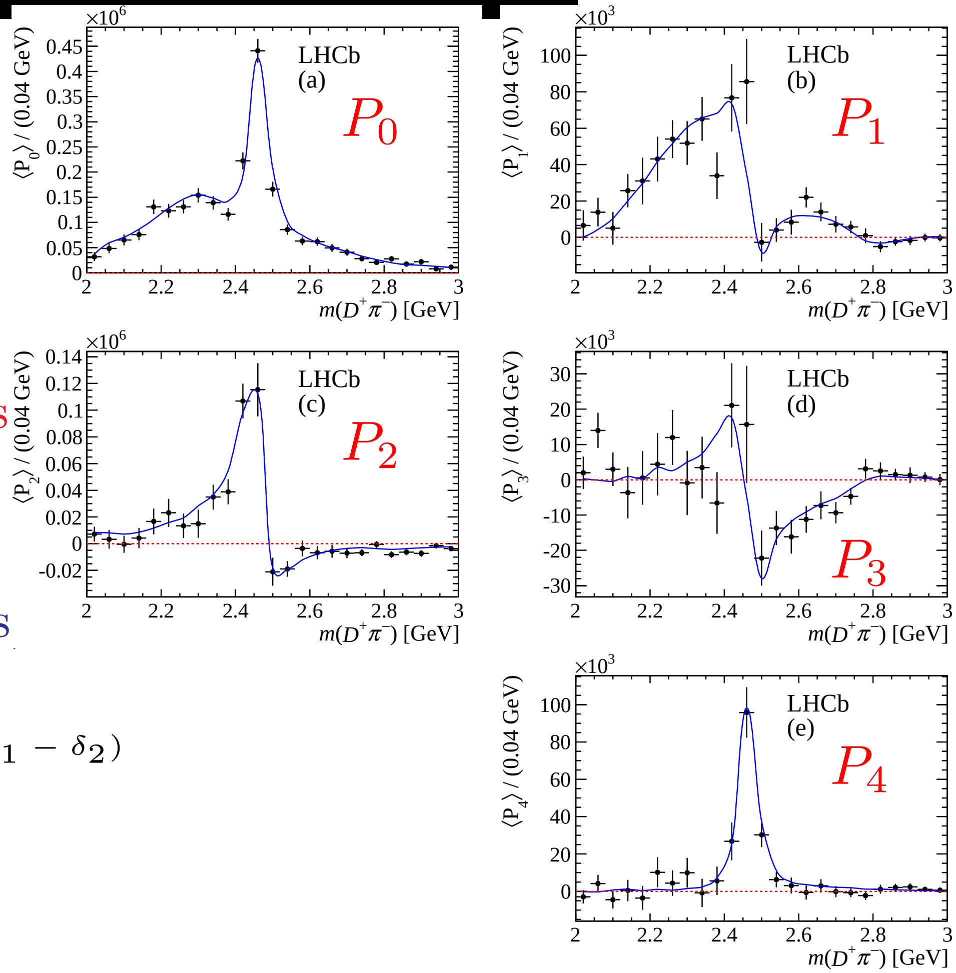

$$\langle P_0 \rangle \propto |h_0|^2 + |h_1|^2 + |h_2|^2$$
$$\langle P_1 \rangle \propto \frac{2}{\sqrt{3}} |h_0||h_1| \cos(\delta_0 - \delta_1) + \frac{4}{\sqrt{15}} |h_1||h_2| \cos(\delta_1 - \delta_2)$$
$$\langle P_2 \rangle \propto \frac{2}{\sqrt{5}} |h_0||h_2| \cos(\delta_0 - \delta_2) + \frac{2}{5} |h_1|^2 + \frac{2}{7} |h_2|^2$$
$$\langle P_3 \rangle \propto \frac{6}{7}\sqrt{\frac{3}{5}} |h_1||h_2| \cos(\delta_1 - \delta_2)$$
$$\langle P_4 \rangle \propto \frac{2}{7} |h_2|^2$$

- P_1 shows the S-P interference.
- P_3 shows the P-D interference.
- Clear D-wave in P_4 due to the $D_2^*(2460)$.

Dalitz plot analysis of $B^- \to D^+ K^- \pi^-$.

- ☐ The Dalitz plot. (arXiv:1503.02995)
- ☐ Need to introduce virtual $D_v^*(2007)^0$ B_v^{*0} and Nonresonant contributions.
- ☐ Clear spin-2 $D_2^*(2460)$ signal.
- ☐ A $D_J^*(2760)^0$ spin-1 resonance.

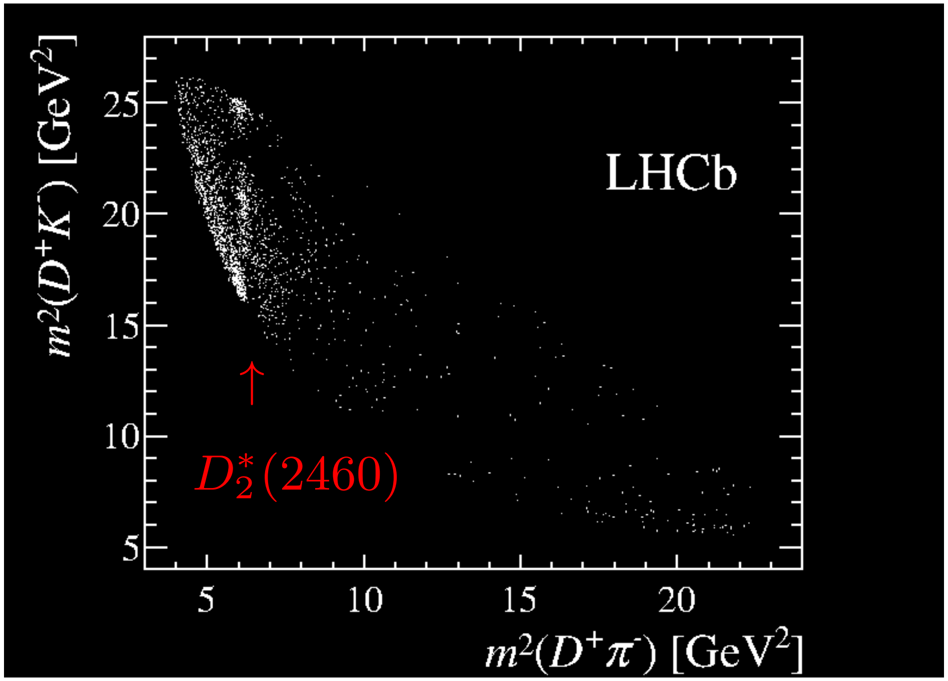

Resonance	Spin	Parameters
$D_0^*(2400)^0$	0	PDG
$D_2^*(2460)^0$	2	$m = 2464.0 \pm 1.4\ MeV,\ \Gamma = 43.8 \pm 2.9\ MeV$
$D_J^*(2760)^0$	1	$m = 2781 \pm 18\ MeV,\ \Gamma = 177 \pm 32\ MeV$
Nonresonant	0	$R_0(m) = e^{-\alpha m^2}$
Nonresonant	1	$R_1(m) = e^{-\beta m^2}$

Dalitz plot analysis of $B^- \to D^+ K^- \pi^-$.

□ $D^+\pi^-$ fit projection (arXiv:1503.02995).

Resonance	Fit fraction
$D_0^*(2400)^0$	$8.3 \pm 2.6 \pm 0.6 \pm 1.9$
$D_2^*(2460)^0$	$31.8 \pm 1.5 \pm 0.9 \pm 1.4$
$D_1^*(2760)^0$	$4.9 \pm 1.2 \pm 0.3 \pm 0.9$
S-wave nonresonant	$38.0 \pm 7.4 \pm 1.5 \pm 10.8$
P-wave nonresonant	$23.8 \pm 5.6 \pm 2.1 \pm 3.7$
$D_v^*(2007)^0$	$7.6 \pm 2.3 \pm 1.3 \pm 1.5$
B_v^*	$3.6 \pm 1.9 \pm 0.9 \pm 1.6$

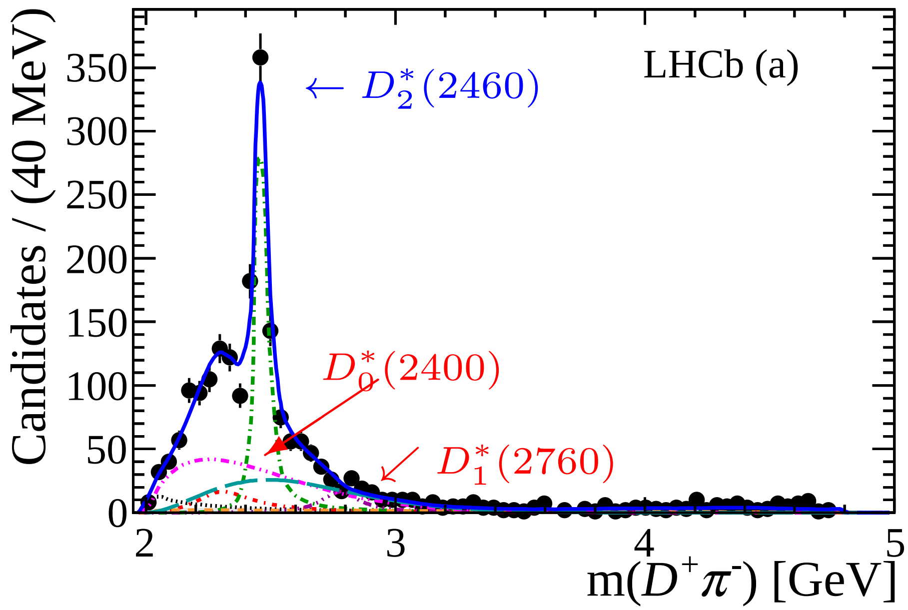

Errors are statistical, systematic and model.

□ The Dalitz analysis of $B^0 \to \bar{D}^0\pi^+\pi^-$ gives evidence for a $D_3^*(2760)$ spin-3 resonance.

□ This state is not observed in this B^- decay channel.

Dalitz plot analysis of $B^0 \to \bar{D}^0\pi^+\pi^-$

(arXiv:1505.01710)

- ☐ $B^0 \to \bar{D}^0\pi^+\pi^-$ mass spectrum.
- ☐ Green line is background.
- ☐ Integrated luminosity: 3 fb^{-1}.

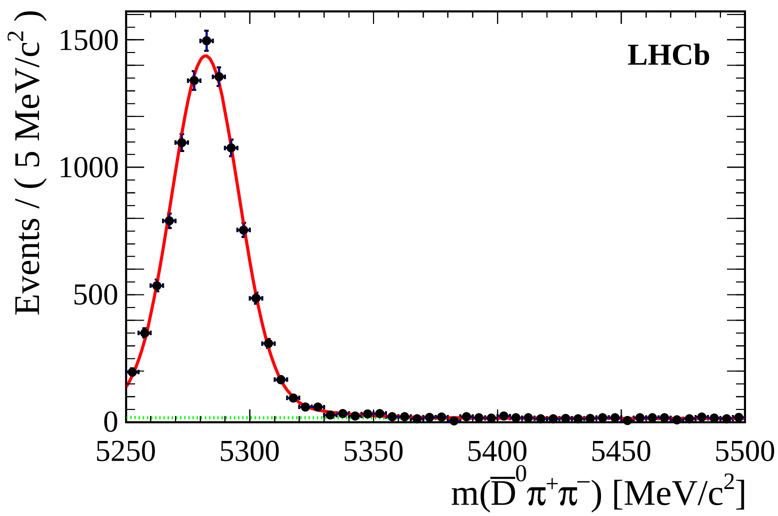

- ☐ 9565 events with 97.8% purity.
- ☐ Dalitz plot.

- ☐ Presence of resonant structure along the $\pi^+\pi^-$ and $\bar{D}^0\pi^-$ axis.
- ☐ Clear spin-2 $D_2^*(2460)$ signal.
- ☐ Clear spin-1 $\rho(770)$ signal.

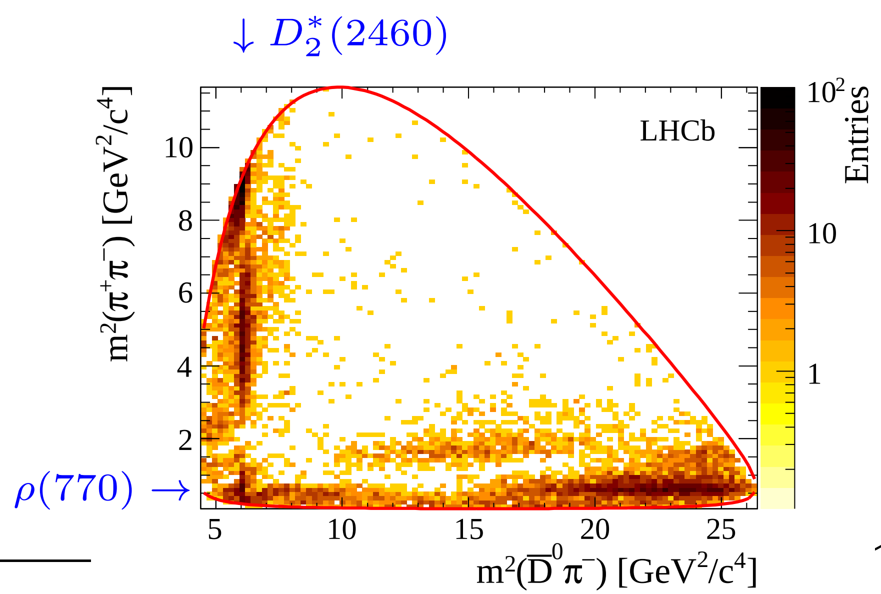

Dalitz plot analysis of $B^0 \to \bar{D}^0\pi^+\pi^-$

□ Analysis performed using the isobar model and a K-matrix description of the $\pi^+\pi^-$ S-wave. Both methods give a good description of the data.

□ $m^2(\pi^+\pi^-)$ fit projections.

□ Signal of ρ/ω interference.

□ Amplitudes fractions.

Errors are statistical, systematic and model.

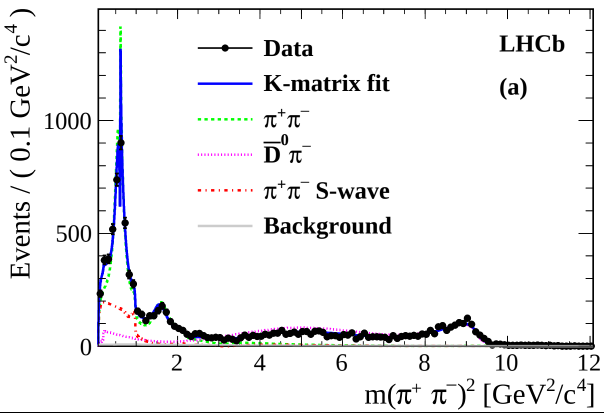

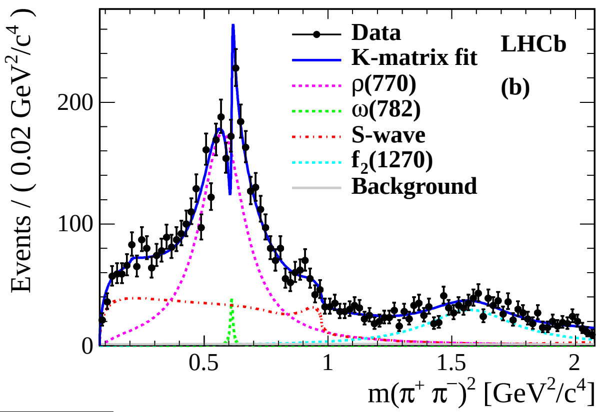

Resonance	Isobar ($\mathcal{F}_i$ %)	K-matrix ($\mathcal{F}_i$ %)
$f_0(500)$	$13.2 \pm 0.89 \pm 0.31 \pm 2.45$	n/a
$f_0(980)$	$1.56 \pm 0.29 \pm 0.11 \pm 0.54$	n/a
$f_0(2020)$	$1.58 \pm 0.36 \pm 0.15 \pm 1.00$	n/a
S-wave	$16.39 \pm 0.58 \pm 0.43 \pm 1.46$	$16.51 \pm 0.70 \pm 1.68 \pm 1.10$
$\rho(770)$	$37.54 \pm 1.00 \pm 0.61 \pm 0.98$	$36.15 \pm 1.00 \pm 2.13 \pm 0.79$
$\omega(782)$	$0.49 \pm 0.13 \pm 0.01 \pm 0.03$	$0.50 \pm 0.13 \pm 0.01 \pm 0.02$
$\rho(1450)$	$1.54 \pm 0.32 \pm 0.08 \pm 0.22$	$2.16 \pm 0.42 \pm 0.82 \pm 0.21$
$\rho(1700)$	$0.38\,^{+0.25}_{-0.12} \pm 0.07 \pm 0.06$	$0.83 \pm 0.21 \pm 0.61 \pm 0.12$
$f_2(1270)$	$10.28 \pm 0.49 \pm 0.31 \pm 1.10$	$9.88 \pm 0.58 \pm 0.83 \pm 0.58$

Dalitz plot analysis of $B^0 \to \bar{D}^0 \pi^+ \pi^-$

- $\bar{D}^0\pi^-$ fit projections (arXiv:1505.01710).

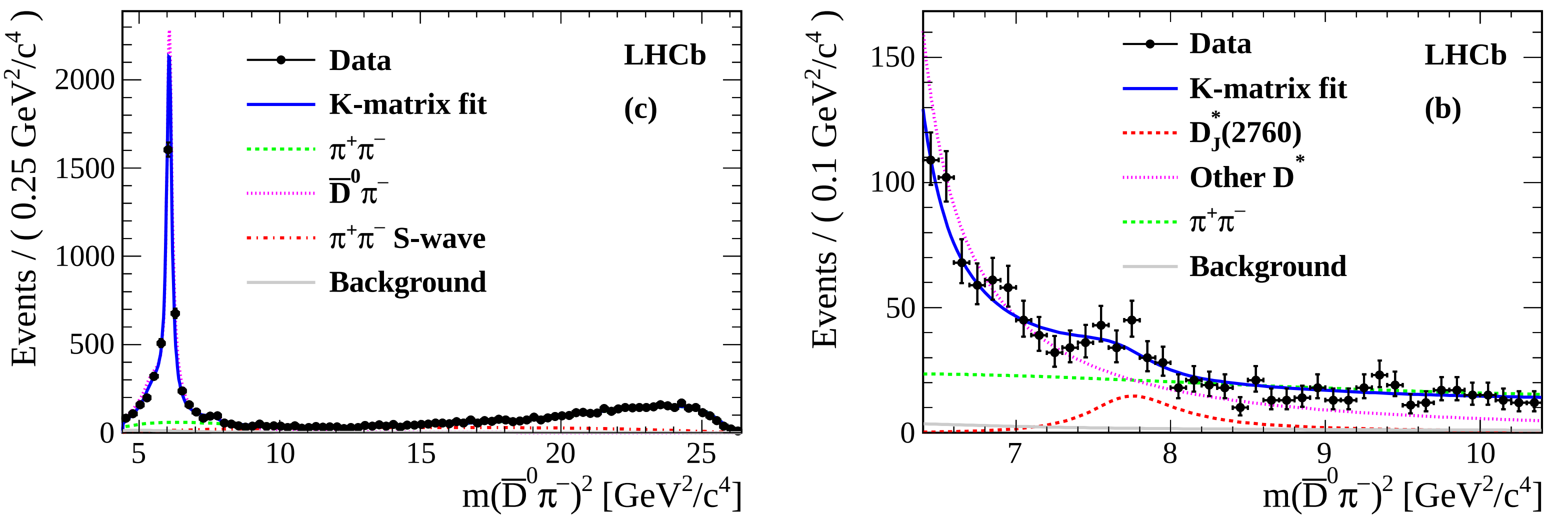

- Amplitudes fractions.

Resonance	Isobar ($\mathcal{F}_i$ %)	K-matrix ($\mathcal{F}_i$ %)
$\bar{D}^0\pi^-$ P-wave	$9.21 \pm 0.56 \pm 0.24 \pm 1.73$	$9.22 \pm 0.58 \pm 0.67 \pm 0.75$
$D_0^*(2400)^-$	$9.00 \pm 0.60 \pm 0.20 \pm 0.35$	$9.27 \pm 0.60 \pm 0.86 \pm 0.52$
$D_2^*(2460)^-$	$28.83 \pm 0.69 \pm 0.74 \pm 0.50$	$28.13 \pm 0.72 \pm 1.06 \pm 0.54$
$D_3^*(2760)^-$	$1.22 \pm 0.19 \pm 0.07 \pm 0.09$	$1.58 \pm 0.22 \pm 0.18 \pm 0.07$

- Observation of a $J^P = 3^-$ resonance.

Dalitz plot analysis of $B^0 \to \bar{D}^0\pi^+\pi^-$

□ Charmed resonances parameters.

		Isobar	K-matrix
$D_0^*(2400)$	m	$2349 \pm 6 \pm 1 \pm 4$	$2354 \pm 7 \pm 11 \pm 2$
	Γ	$217 \pm 13 \pm 5 \pm 12$	$230 \pm 15 \pm 18 \pm 11$
$D_2^*(2460)$	m	$2468.6 \pm 0.6 \pm 0.0 \pm 0.3$	$2468.1 \pm 0.6 \pm 0.4 \pm 0.3$
	Γ	$47.3 \pm 1.5 \pm 0.3 \pm 0.6$	$46.0 \pm 1.4 \pm 1.7 \pm 0.4$
$D_3^*(2760)$	m	$2798 \pm 7 \pm 1 \pm 7$	$2802 \pm 11 \pm 10 \pm 3$
	Γ	$105 \pm 18 \pm 6 \pm 23$	$154 \pm 27 \pm 13 \pm 9$

□ Summary of $D_J^*(2760)$ parameters.

□ Presence of overlapping $J^P = 1^-$ and $J^P = 3^-$ resonances?

□ Inclusive data cannot separate the two contributions.

□ These two states are expected to be close in mass.

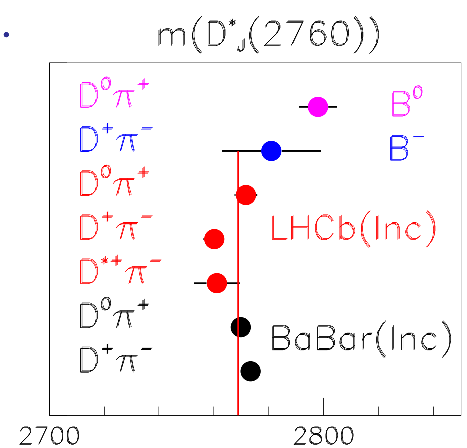

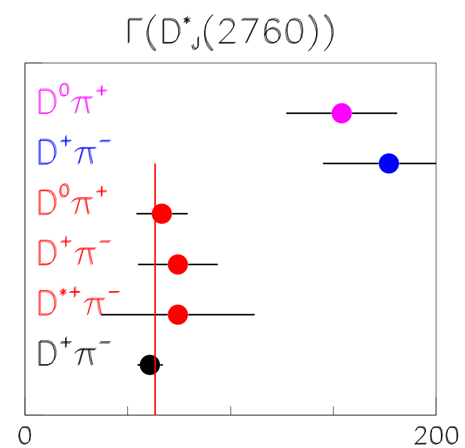

Dalitz plot analysis of $B^0 \to \bar{D}^0 K^+ \pi^-$

(arXiv:1505.01505)

- ☐ 2344 events in the B^0 signal region.
- ☐ Integrated luminosity: 3 fb^{-1}.

- ☐ B^0 Dalitz plot.
- ☐ B^0 mass constraint is applied in the Dalitz plot analysis.

- ☐ New parameters have been obtained for the broad $D_0^*(2400)$ resonance.

Final state	Method	Mass	Width
$B^0 \to \bar{D}^0 K^+ \pi^-$	Free	2360 ± 15	255 ± 26
$B^0 \to \bar{D}^0 \pi^+ \pi^-$	Free	2354 ± 7	230 ± 15
$B^- \to D^+ K^- \pi^-$	(PDG)	2318 ± 29	267 ± 40

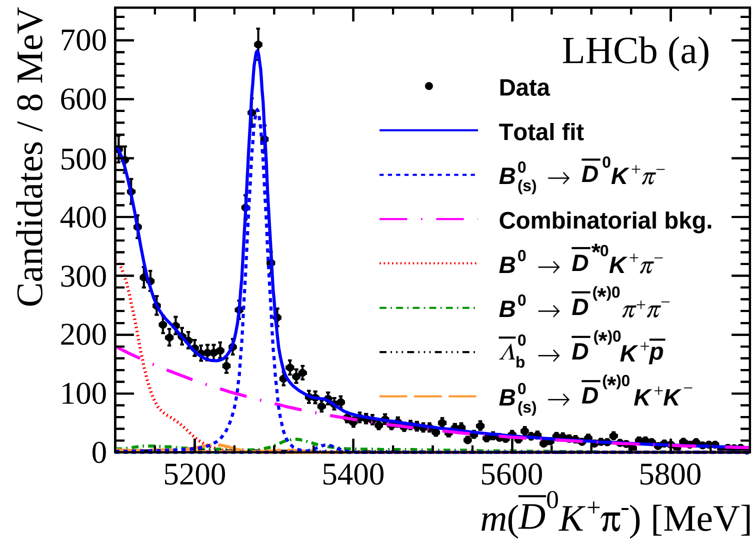

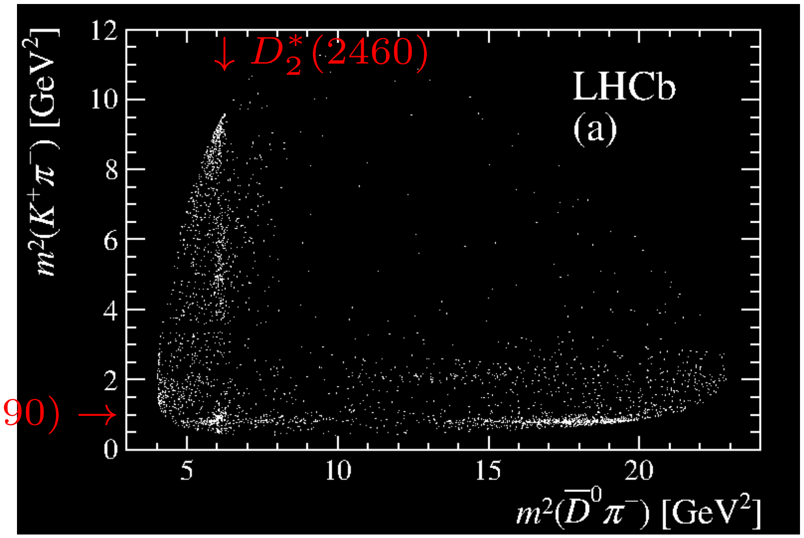

Dalitz plot analysis of $B^0 \to \bar{D}^0 K^+ \pi^-$

□ Results from the Dalitz plot analysis and fit projections (arXiv:1505.01505).

Resonance	Fit fraction (%)
$K^*(892)^0$	37.4 ± 1.5
$K^*(1410)^0$	0.7 ± 0.3
$K_0^*(1430)^0$	5.1 ± 2.0
$K\pi$ S-wave LASS nonresonant	4.8 ± 3.8
LASS total	6.7 ± 2.7
$K_2^*(1430)^0$	7.4 ± 1.7
$D_0^*(2400)^-$	19.3 ± 2.8
$D_2^*(2460)^-$	23.1 ± 1.2
$D\pi$ S-wave (nonresonant)	6.6 ± 1.4
$D\pi$ P-wave (Form Factor)	8.9 ± 1.6
Total fit fraction	113.4

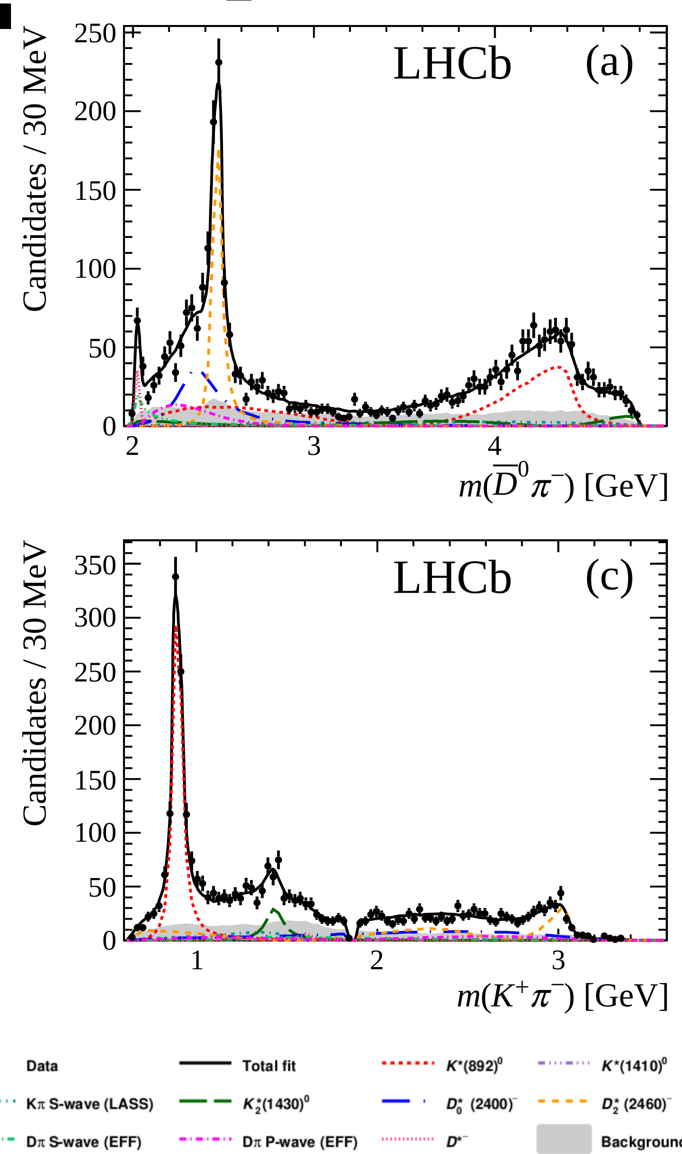

□ No evidence is found for additional spin-1 or spin-3 D_J^* resonances.

Experimental and theoretical status of the D_s mesons.

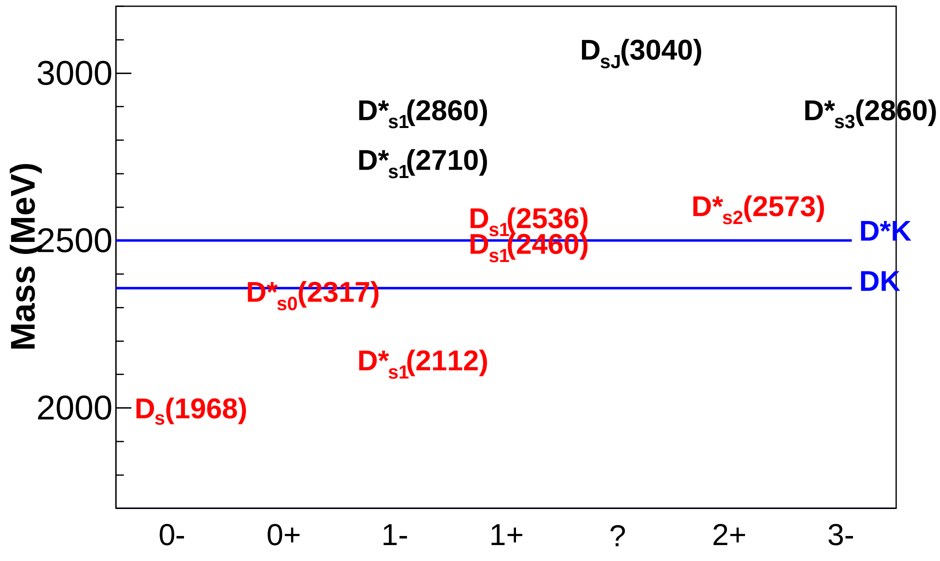

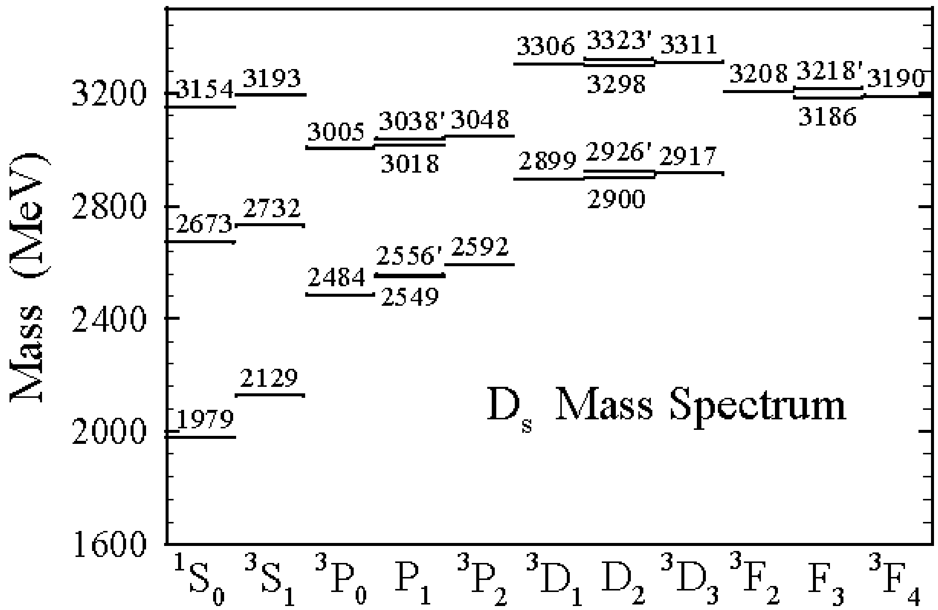

□ Several new states (in black) recently discovered in the DK and D^*K mass spectra.

□ Recent calculation of the $c\bar{s}$ spectrum S. Godfrey and I.T. Jardine(arXiv:1312.6181).

□ Work is in progress to search for new D_s mesons using:

- An inclusive approach:

$$pp \to D_{sJ} X$$

- From Dalitz plot analyses of B and B_s decays.

Observation of $D_{s1}^*(2710)^+$ and $D_{sJ}^*(2860)^+$ in LHCb.

□ Obtain 0.36×10^6 $D^+K_S^0$ and 3.15×10^6 D^0K^+ inclusive candidates. 1 fb^{-1} (JHEP 1210 (2012) 151).

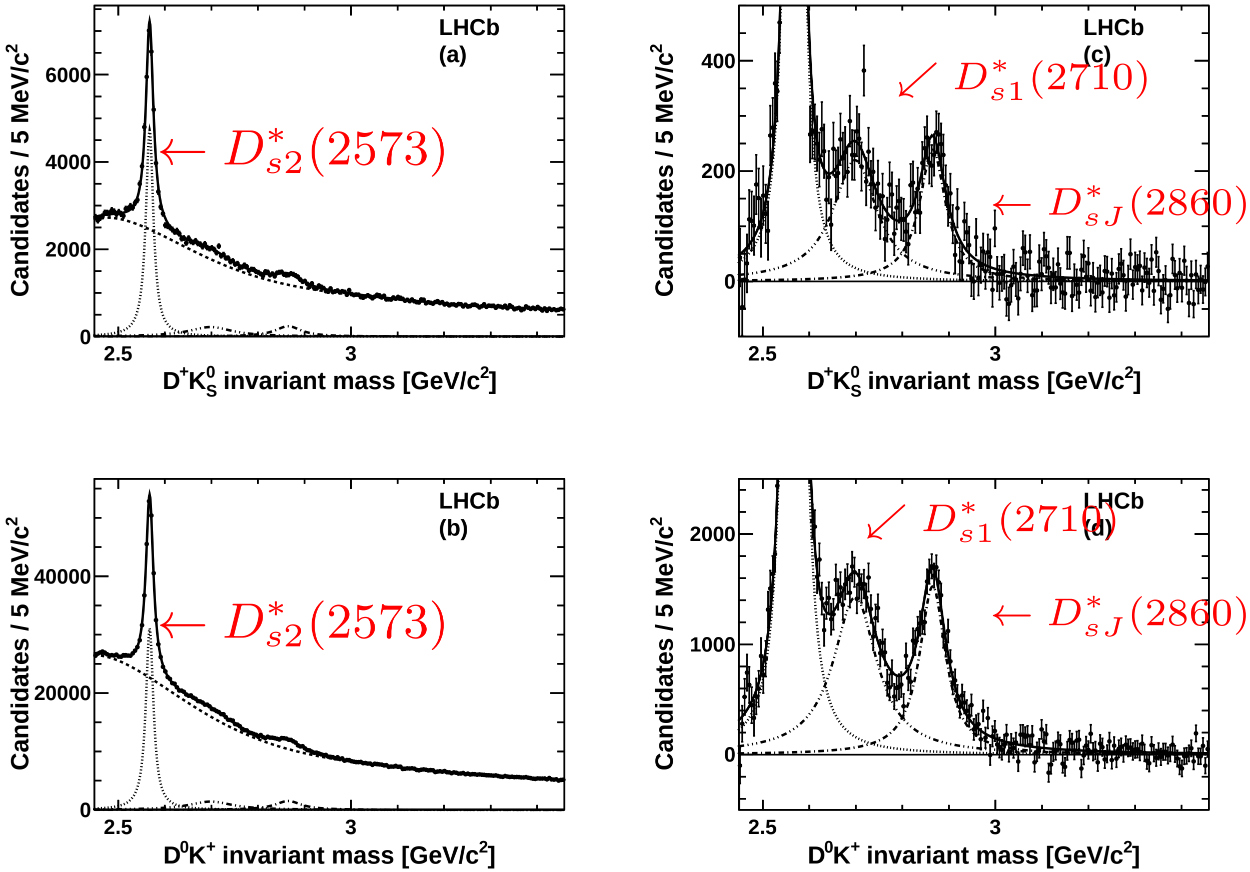

□ Observation of $D_{s2}^*(2573)$, $D_{s1}^*(2710)$, and $D_{sJ}^*(2860)$.

Dalitz plot analysis of $B_s^0 \to \bar{D}^0 K^- \pi^+$.

□ $\bar{D}^0 K^- \pi^+$ mass spectrum

(Phys. Rev. D 90, 072003 (2014)) .

□ 11302 ± 159 signal events.

□ 3 fb^{-1} integrated luminosity.

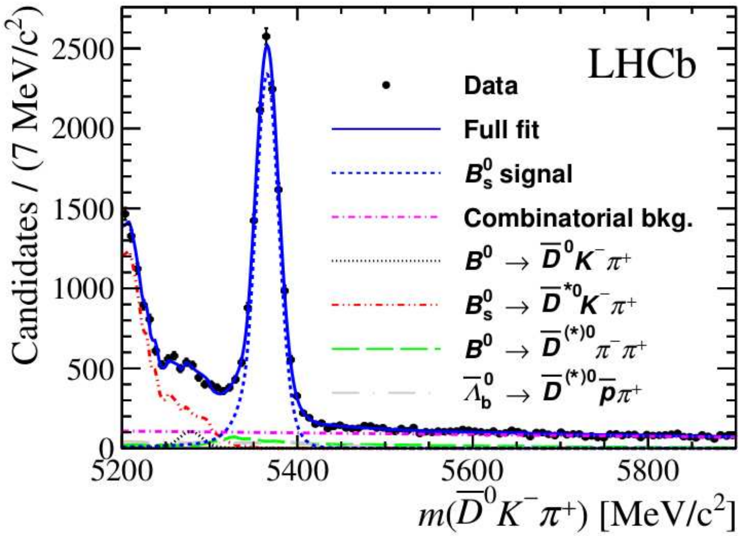

$\downarrow D_{s2}^*(2573)$

□ The largest components are:

$\bar{\mathrm{K}}^*(892)^0$ (28.6 %),

$D_{s2}^*(2573)^-$ (25.7 %),

$K\pi$ S-wave (LASS) (21.4 %)

$\bar{D}^0 K^-$ nonresonant (12.4 %).

$\bar{\mathrm{K}}^*(892)^0 \rightarrow$

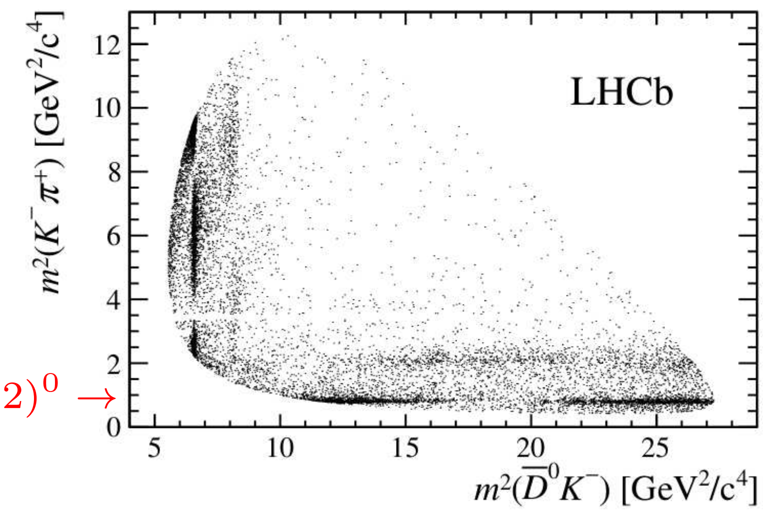

Dalitz plot analysis of $B_s \to \bar{D}^0 K^- \pi^+$.

□ Fit projections.

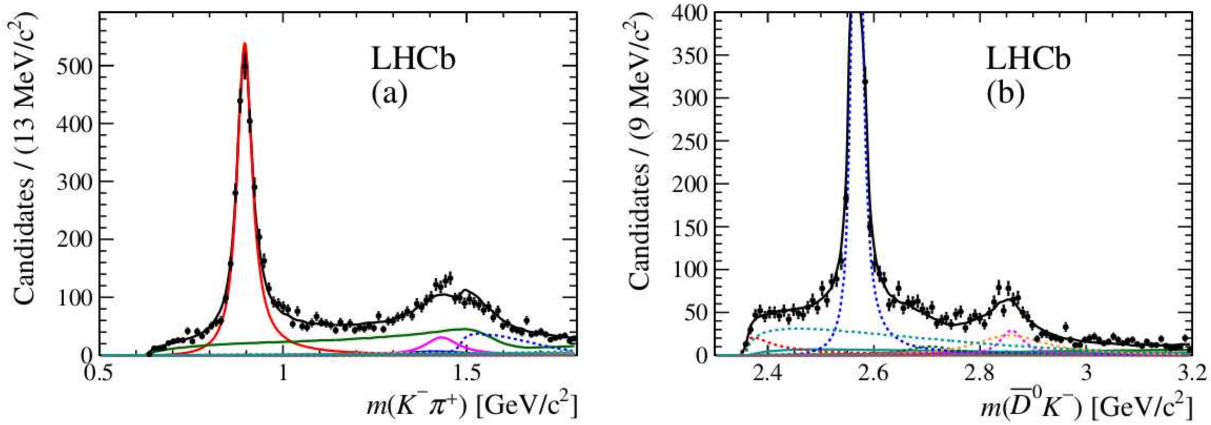

□ Signal present in the 2860 MeV $\bar{D}^0 K^-$ mass region described by a superposition of
a spin-1 $(5.0 \pm 1.2 \pm 0.7 \pm 3.3)\,\%$
and a spin-3 $(2.2 \pm 0.1 \pm 0.3 \pm 0.4)\,\%$ resonance.

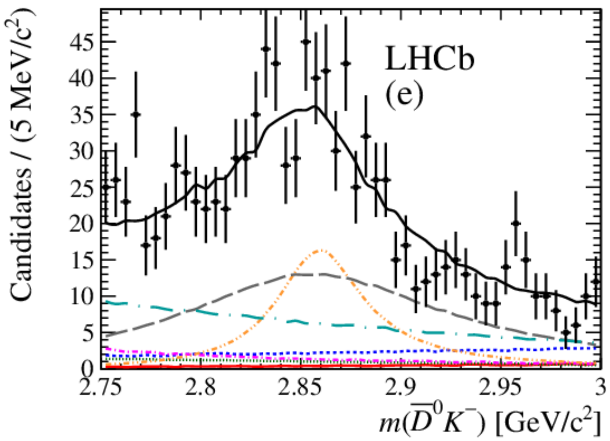

□ Resonances parameters:

$$m(D^*_{s1}(2860)^-) = 2859 \pm 12 \pm 6 \pm 23\,\text{MeV}/c^2, \Gamma(D^*_{s1}(2860)^-) = 159 \pm 23 \pm 27 \pm 72\,\text{MeV}/c^2$$

$$m(D^*_{s3}(2860)^-) = 2860.5 \pm 2.6 \pm 2.5 \pm 6.0\,\text{MeV}/c^2, \Gamma(D^*_{s3}(2860)^-) = 53 \pm 7 \pm 4 \pm 6\,\text{MeV}/c^2$$

Determination of the $X(3872) \to J/\psi\rho(770)$ quantum numbers.

□ We study the decay $B^+ \to X(3872)K^+$ with $X(3872) \to J/\psi\pi^+\pi^-$ (arXiv:1504.06339).

□ The quantum numbers of $X(3872) \to J/\psi\rho(770)$ have been determined to be $J^{PC} = 1^{++}$.

□ However it was assumed that the decay is dominated by the lowest values of angular momentum between the $X(3872)$ decay products.

□ The analysis is repeated here using 3-times the statistics and without any assumption on L_{min}.

□ $N(B^+ \to X(3872)K^+) = 1011 \pm 38$ with 80% signal purity.

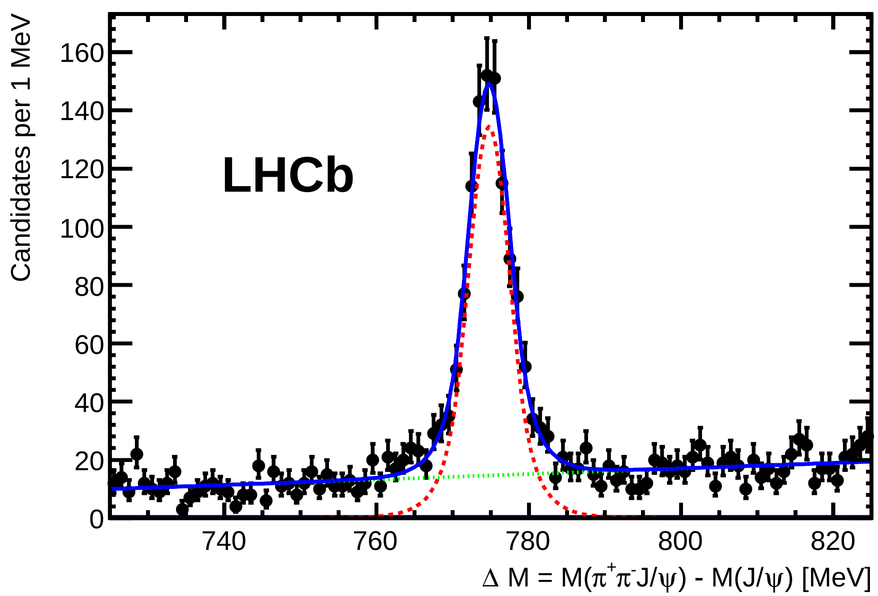

Determination of the $X(3872) \to J/\psi\rho(770)$ quantum numbers.

□ Distributions of the test statistic $t \equiv -2\ln[Ł(J_X^{alt}))/Ł(1^{++})]$, for the simulated experiments under the $J^{PC} = J_X^{alt}$ hypothesis and under the $J^{PC} = 1^{++}$ hypothesis.

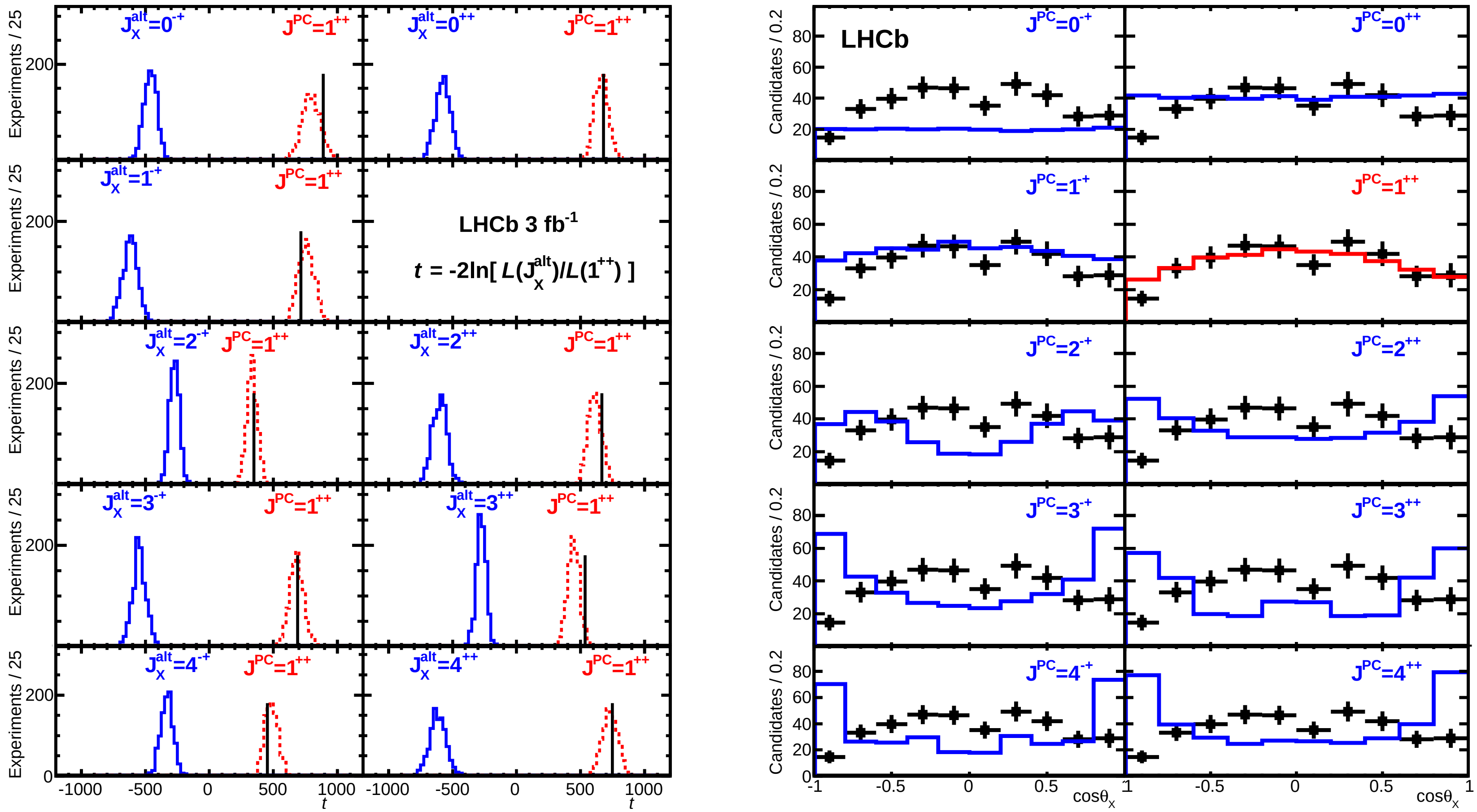

□ $J^{PC} = 1^{++}$ gives the highest Likelihood value with an upper limit of D-wave contribution of 4% at 95% C.L.

Summary.

- Many new D_J and D_{sJ} mesons observed in both inclusive and exclusive B/B_s decays.
- The observation of these states in B/B_s decays allows the determination of their quantum numbers.
- New high statistics data will be shortly available and new decay channels will be analyzed. These studies will allow to better understand the charm and strange-charm spectrum.
- The quantum numbers of $X(3872)$ are established to be $J^{PC} = 1^{++}$ without any assumption on the orbital angular momentum in the decay.